Laboratory Investigation

BASF DocID 2006/1052493

Vascular Anatomic Variation in Rabbits

Yong Hong Ding, MD, Daying Dai, MD, Kennith F. Layton, MD, Debra A. Lewis, PhD, Mark A. Danielson, PhD, Ramanathan Kadirvel, PhD, Harry J. Cloft, MD, PhD, and David F. Kallmes, MD

PURPOSE: To explore the vascular anatomic variation along the aortic arch in New Zealand White rabbits with the goal of highlighting potential anatomic configurations that might be encountered in the performance of preclinical endovascular research in rabbits.

MATERIALS AND METHODS: Digital subtraction angiography images of the brachiocephalic artery (BCA) and aortic arch in New Zealand White rabbits were obtained after creation of elastase-induced aneurysms at the origin of the right common carotid artery (RCCA) in 214 animals. The patterns of origin of the RCCA and left common carotid artery (LCCA), right subclavian artery (RSCA) and left subclavian artery (LSCA), and right vertebral artery (RVA) and left vertebral artery (LVA) were analyzed.

RESULTS: Five predominant variations of vessel origin were identified. In 200 of 214 cases (93%), the LCCA originated from the bifurcation of the BCA and aorta. In eight cases (4%), the LCCA directly originated from the aorta. In two cases (1%), the LCCA originated from the BCA. Aberrant RSCA anatomy in which the RSCA originated from the aortic arch instead of the BCA was found in three cases (1.5%). In a single case (0.5%), aberrant RSCA anatomy with the RVA originating from the BCA was encountered.

CONCLUSIONS: Anatomic variation of the BCA in New Zealand White rabbits is similar to that seen in humans. Understanding of the normal and variant anatomy of the rabbit will aid investigators who use the rabbit model for endovascular research.

J Vasc Interv Radiol 2006; 17:1031–1035

Abbreviations: BCA = brachiocephalic artery, DSA = digital subtraction angiography, LCCA = left common carotid artery, LSCA = left subclavian artery, RCCA = right common carotid artery, RSCA = right subclavian artery

THE rabbit elastase-induced carotid aneurysm model has been used widely, especially for testing of new neurovascular devices (1–11). This model coverts the origin of the right common carotid artery (RCCA) into an aneurysmal sac after distal ligation and intraluminal incubation of elastase. We have encountered anatomic variations in rabbits such as origin of the left common carotid artery (LCCA) from the brachiocephalic artery (BCA), as seen along the aortic arch in humans, which may complicate creation or embolization of these model aneurysms.

In this study, we evaluated and catalogued the vascular origination of the major brachiocephalic vessels (including the RCCA and LCCA, right subclavian artery [RSCA] and left subclavian artery [LSCA], and right vertebral artery [RVA] and left vertebral artery [LVA]) from the aortic arch. In this article, we report the details of each anatomic variant and discuss their relevance regarding experimental aneurysm creation. In addition, we compare variant anatomy in rabbits with that in humans. All these anatomic findings should be applicable not only to experimental aneurysm research but also to investigators who (i) introduce catheters into carotid arteries for distal (ie, iliac) artery interventions and (ii) perform retrograde catheterizations of the carotid arteries for angioplasty studies or more distal cerebral catheterizations.

MATERIALS AND METHODS

Aneurysm Creation

In all, 214 elastase-induced aneurysms in New Zealand White rabbits were analyzed. All procedures were approved by the institutional animal care and use committee at our institution. Detailed procedures for aneurysm creation have been described (1). Briefly, New Zealand White rabbits (3–4 kg) were anesthetized with intramuscular injection of ketamine, xylazine, and acepromazine (75 mg/kg, 5 mg/kg, and 1 mg/kg, respectively). With sterile technique, a 5-F sheath (Cordis, Miami Lakes, FL) was ad-

From the Neuroradiology Research Laboratory, Department of Radiology, Mayo Clinic, 200 First Street, Southwest, Rochester, Minnesota 55905. Received December 28, 2005; revision requested; final revision received and accepted March 13, 2006. **Address correspondence to** D.F.K.; E-mail: kallmes.david@mayo.edu

This study was supported by NIH grant NS42646. None of the authors have identified a conflict of interest.

© SIR, 2006

DOI: 10.1097/01.RVI.0000220677.34695.29

Copyright © by the Society of Interventional Radiology. Unauthorized reproduction of this article is prohibited.

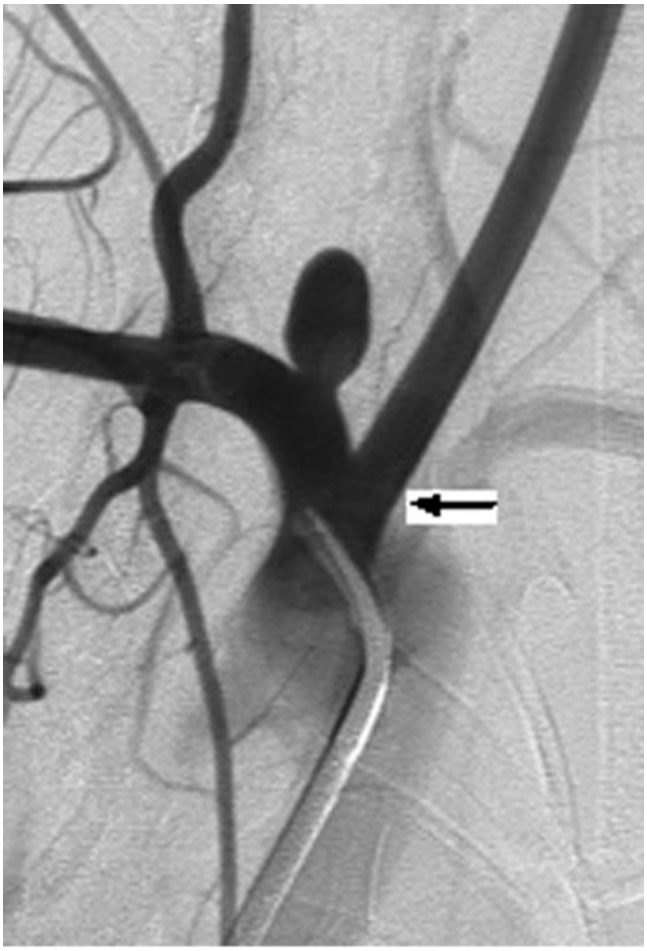

1.

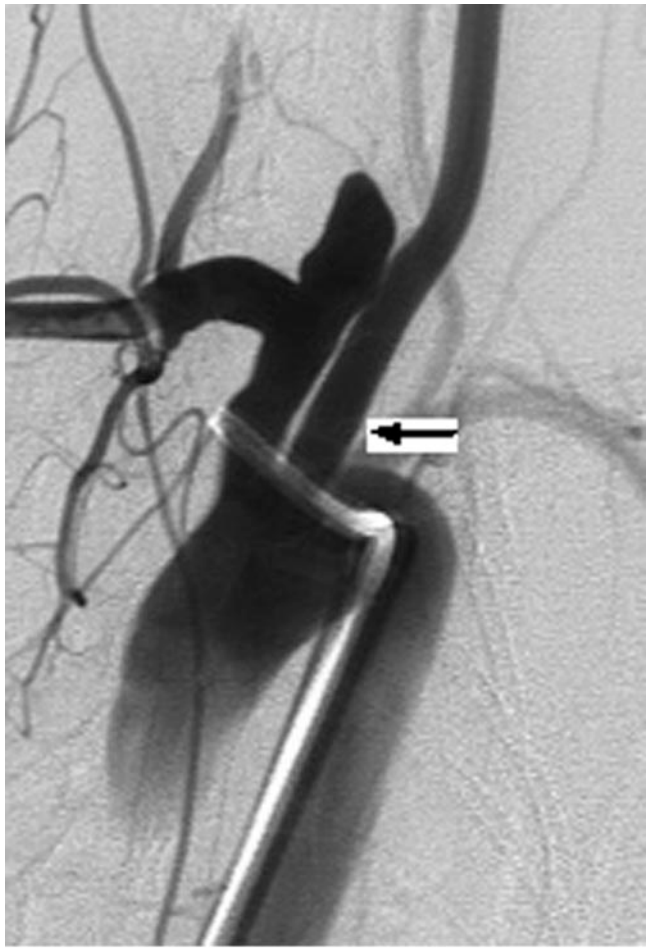

2.

Figures 1, 2. **(1)** Right anterior oblique DSA image of the BCA. The LCCA originates from the bifurcation of the BCA and the aorta (black arrow). **(2)** Right anterior oblique DSA image of the BCA. The LCCA originates separately from the aortic arch (black arrow).

vanced in a retrograde fashion in the RCCA to a point approximately 3 cm cephalad to the origin of the RCCA. A 3-F Fogarty balloon (Baxter, Irvine, CA) was inflated to achieve flow arrest in the RCCA. Porcine elastase mixed with iodinated contrast material was incubated in the "dead space" of the RCCA above the inflated balloon for 20 minutes.

Follow-up Angiography

Digital subtraction angiography (DSA) images of the brachiocephalic artery (BCA) and the surrounding major vessels for each aneurysm before endovascular treatment were analyzed. Detailed methods of DSA have been described elsewhere (4). Briefly, with use of sterile technique, surgical exposure of the right common femoral artery was performed, and a 5-F vascular sheath was placed. The side port of the sheath was flushed with heparinized saline solution, and then a bolus of heparin (100 U/kg) was delivered through the sheath. A 5-F Envoy catheter (Cordis) was advanced into the origin of the BCA or the aortic arch through the sheath under fluoroscopic guidance (Advantx; General Electric Medical Systems; Milwaukee, WI). DSA at 2 frames/sec was performed with a hand injection of 5 mL of iodinated contrast material (Omnipaque 300; Amersham, Princeton, NJ) at a rate of approximately 3 mL/sec in the right anterior oblique view.

From the DSA images, we determined the pattern of origin of the RCCA and LCCA, the RSCA and LSCA, and the RVA and LVA. Dominant patterns were identified, and the frequency of each variant was calculated.

RESULTS

Five predominant variations of vessel origin were identified. These configurations are shown in **Figures 1–5**.

Type 1

In type 1 anatomy, the LCCA originates from the bifurcation of the BCA and the aortic arch. This anatomic type was identified in 200 of 214 animals (93%). The RSCA originated from the BCA, and the RVA originated from the RSCA (**Fig 1**).

Copyright © by the Society of Interventional Radiology. Unauthorized reproduction of this article is prohibited.

3.

4.

Figures 3, 4. **(3)** Right anterior oblique DSA image of the BCA. The LCCA originates from the BCA (black arrow). **(4)** Right anterior oblique DSA image of the aortic arch. Aberrant RSCA anatomy in which the RSCA originates from the aortic arch distal to the LSCA (black arrow). The RVA originates from the aberrant RSCA (white arrow).

Type 2

In type 2 anatomy, there are separate origins of the LCCA and the RCCA from the aortic arch. Eight cases (4%) showed that the LCCA directly originated from the aortic arch, separately from the BCA. The RSCA originated from the BCA and the RVA originated from the RSCA (**Fig 2**).

Type 3

In type 3 anatomy, the LCCA originates from the BCA. The LCCA originated from the BCA in two cases in this study (1%). In these cases, the RSCA originated from the BCA and the RVA originated from the RSCA (**Fig 3**).

Type 4

In type 4 anatomy, there is an aberrant RSCA, with the RVA originating from the RSCA. We noted three cases (1.5%) in which the RSCA originated as a separate branch from the aortic arch distal to the LSCA, with the RVA branching from the aberrant RSCA. This configuration is generally known as aberrant RSCA anatomy (**Fig 4**).

Type 5

In type 5 anatomy, there is an aberrant RSCA ,with the RVA originating from the BCA. In a single case (0.5%), aberrant RSCA anatomy was noted in which the RVA originated from the BCA rather than from the aberrant RSCA (**Fig 5**).

In all cases, the RCCA originated from the BCA, the LSCA originated from the aortic arch, and the LVA originated from the LSCA.

DISCUSSION

The rabbit elastase-induced aneurysm model has been accepted as a useful model for testing neurovascular devices (12–17). However, few vascular anatomic studies of the aortic arches of rabbits have been reported (18). The anatomy described as type 1 in this study is most frequently encountered in rabbits, which is consistent with the findings of other researchers (19).

Anatomic variations shown in this study may affect the safety and feasibility of aneurysm creation and aneu-

Copyright © by the Society of Interventional Radiology. Unauthorized reproduction of this article is prohibited.

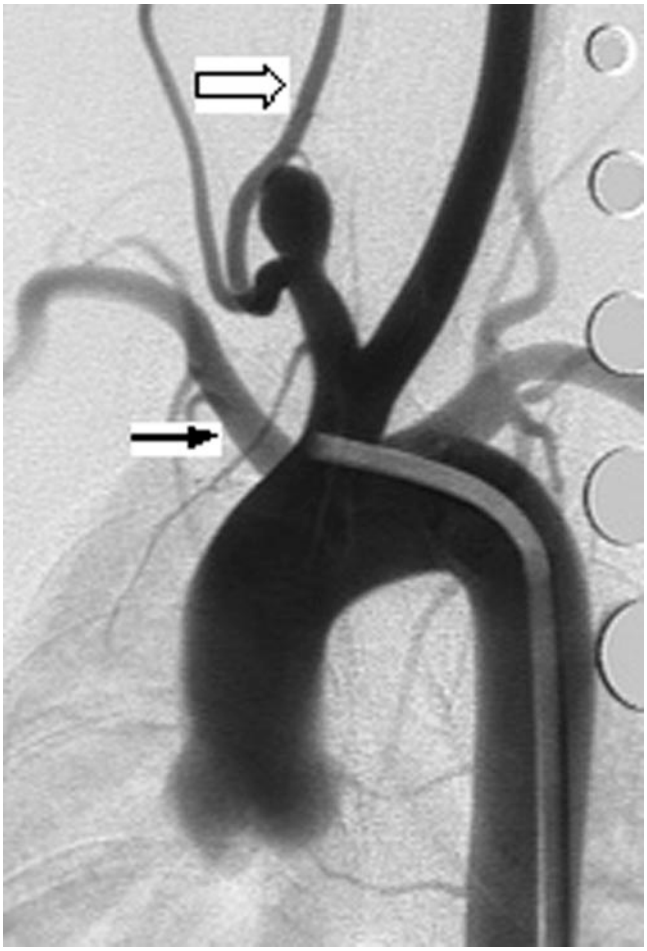

Figure 5. Right anterior oblique DSA image of the aortic arch shows aberrant RSCA anatomy (black arrow). The RVA originates from the BCA (white arrow).

rysm embolization in rabbit aneurysm models. These results should also be useful for other relative experimental research involving major branches from the aortic arch when a rabbit model is used. Aneurysm creation includes placement of an occlusion balloon across the origin of the RCCA to incubate elastase in the lumen of the RCCA. In cases of LCCA origin from the BCA, placement of the occlusion balloon may result in profound ischemia of the face and head. In addition, presence of an aberrant RSCA leads to marked differences in resultant aneurysm anatomy. Instead of originating from the apex of the curve of the BCA as in standard anatomic cases, the aneurysm in cases of an aberrant RSCA originates from the aortic arch. Embolization of this type of aneurysm may be difficult or impossible.

Multiple anatomic variations of the main branches along the aortic arch in humans have been reported (20–25). These include the LVA directly originating from the aortic arch, the LCCA originating from the BCA, the aberrant RSCA, and separate origins of all four major vessels (RSCA, LSCA, RCCA, and LCCA) from the aortic arch. Although the occurrence rates of anatomic variants differ between rabbits and humans, similar anatomic aortic arch variants occur in humans and rabbits. In humans, the most common configuration is a separate origin of the LCCA from the aortic arch (66%), which occurs in 4% of rabbits. The origin of the LCCA from the bifurcation of the BCA and the aortic arch is the most common pattern seen in rabbits (93%) but occurs in only 27% of humans. The LCCA originating from the BCA instead of the aortic arch, which has been described as the "bovine arch" (26), was seen in 1% of rabbits in this study, compared with 7% in humans. An aberrant RSCA occurs in 0.4%–2% of humans, which is similar to the 2% rate encountered in rabbits (25).

References

1. Altes TA, Cloft HJ, Short JG, et al. 1999 ARRS Executive Council Award creation of saccular aneurysms in the rabbit: a model suitable for testing endovascular devices: American Roentgen Ray Society. AJR Am J Roentgenol 2000; 174:349–354.
2. Hoh BL, Rabinov JD, Pryor JC, Ogilvy CS. A modified technique for using elastase to create saccular aneurysms in animals that histologically and hemodynamically resemble aneurysms in human. Acta Neurochirurg 2004; 146: 705–711.
3. Krings T, Moller-Hartmann W, Hans FJ, et al. A refined method for creating saccular aneurysms in the rabbit. Neuroradiology 2003; 45:423–429.
4. Kallmes DF, Helm GA, Hudson SB, et al. Histologic evaluation of platinum coil embolization in an aneurysm model in rabbits. Radiology 1999; 213: 217–222.
5. Hans FJ, Krings T, Moller-Hartmann W, et al. Endovascular treatment of experimentally induced aneurysms in rabbits using stents: a feasibility study. Neuroradiology 2003; 45:430–434.
6. Fujiwara NH, Cloft HJ, Marx WF, et al. Serial angiography in an elastase-induced aneurysm model in rabbits: evidence for progressive aneurysm enlargement after creation. AJNR Am J Neuroradiol 2001; 22:698–703.
7. Short JG, Fujiwara NH, Marx WF, et al. Elastase- induced saccular aneurysms in rabbits: comparison of geometric features with those of human aneurysms. AJNR Am J Neuroradiol 2001; 22:1833–1837.
8. Kallmes DF, Fujiwara NH, Berr SS, et al. Elastase-induced saccular aneurysms in rabbits: a dose-escalation study. AJNR Am J Neuroradiol 2002; 23:295–298.
9. Kallmes DF, Fujiwara NH. New expandable hydrogel-platinum coil hybrid device for aneurysm embolization. AJNR Am J Neuroradiol 2002; 23: 1580–1588.
10. Kallmes DF, Fujiwara NH, Yuen D, et al. A collagen-based coil for embolization of saccular aneurysms in a New Zealand white rabbit model. AJNR Am J Neuroradiol 2003; 24:591–596.
11. Marx WF, Cloft HJ, Helm GA, et al. Endovascular treatment of experimental aneurysms by use of biologically modified embolic devices: coil-mediated intraaneurysmal delivery of fibro-

Copyright © by the Society of Interventional Radiology. Unauthorized reproduction of this article is prohibited.

blast tissue allografts. AJNR Am J Neuroradiol 2001; 22:323–333.
12. De Gast AN, Altes TA, Marx WF, et al. Transforming growth factor beta-coated platinum coils for endovascular treatment of aneurysms: an animal study. Neurosurgery 2001; 49:690–696.
13. Fujiwara NH, Kallmes DF. Healing response in elastase-induced rabbit aneurysms after embolization with a new platinum coil system. AJNR Am J Neuroradiol 2002; 23:1137–1144.
14. Moller-Hartmann W, Krings T, Hans FJ, et al. Endovascular treatment of experimental aneurysms in rabbits using Guglielmi detachable coils: a feasibility study. Neuroradiology 2002; 44: 946–949.
15. Thiex R, Moller-Hartmann W, Hans FJ, et al. Are the configuration and neck morphology of experimental aneurysms predictable? A technical approach. Neuroradiology 2004; 46:571–576.
16. Ding YH, Dai D, Lewis DA, et al. Angiographic and histologic analysis of experimental aneurysms embolized with platinum coils, Matrix, and HydroCoil. AJNR Am J Neuroradiol 2005; 26:1757–1763.
17. Dai D, Ding YH, Danielson MA, et al. Histopathologic and immunohistochemical comparison of human, rabbit, and swine aneurysms embolized with platinum coils. AJNR Am J Neuroradiol 2005; 26:2560–2568.
18. Okuda H, Okada S, Toda I, et al. Three cases of defect of the left common carotid artery in the rabbit. Okajimas Folia Anat Jpn 1988; 65:105–115.
19. Popesko P, Rajtová V, Horák J. A color atlas of anatomy of small laboratory animals, volume one: rabbit/guinea pig, second edition. Philadelphia: WB Saunders; 2002:57.
20. Gluncic V, Lukic IK, Kopljar M, et al. Persistent cervical intersegmental artery and aortic arch coarctation. Surg Radiol Anat 2002; 24:226–230.
21. Dinc H, Alioglu Z, Erdol H, et al. Agenesis of the internal carotid artery associated with aortic arch anomaly in a patient with congenital Horner's syndrome. AJNR Am J Neuroradiol 2002; 23:929–931.
22. Best IM, Bumpers HL. Anomalous origins of the right vertebral, subclavian, and common carotid arteries in a patient with a four-vessel aortic arch. Ann Vasc Surg 2002; 16:231–234.
23. Albayram S, Gailloud P, Wasserman BA. Bilateral arch origin of the vertebral arteries. AJNR Am J Neuroradiol 2002; 23:455–458.
24. Nelson ML, Sparks CD. Unusual aortic arch variation: distal origin of common carotid arteries. Clin Anat 2001; 14:62–65.
25. Osborn AG. Diagnostic cerebral angiography, second edition. Philadelphia: Lippincott Williams & Wilkins; 1999:12–29.
26. Shaw JA, Gravereaux EC, Eisenhauer AC. Carotid stenting in the bovine arch. Catheter Cardiovasc Interv 2003; 60:566–569.

Copyright © by the Society of Interventional Radiology. Unauthorized reproduction of this article is prohibited.